Aalto-yliopisto
Insinööritieteiden korkeakoulu

Deformation II

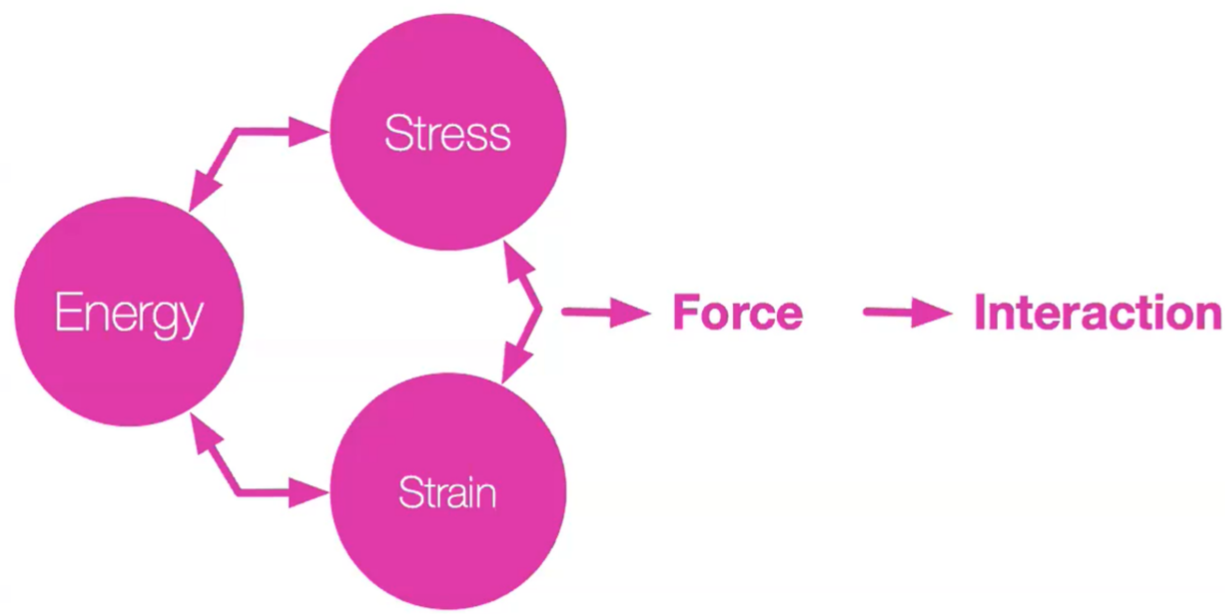

Macroscopic approximation

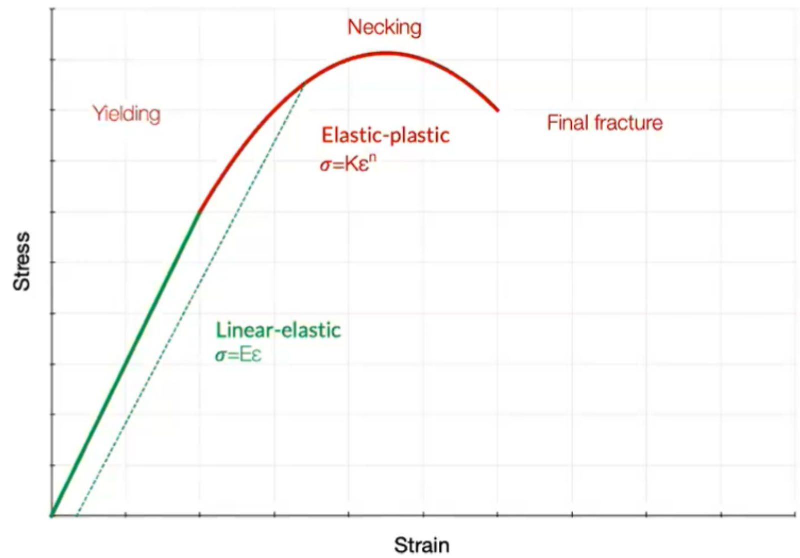

Inhomogenous material

Material has inclusions, precipitates, impurities and lattice defects. These cause stress concentrations in microscopic level.

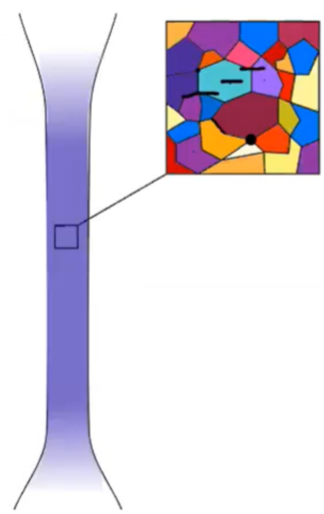

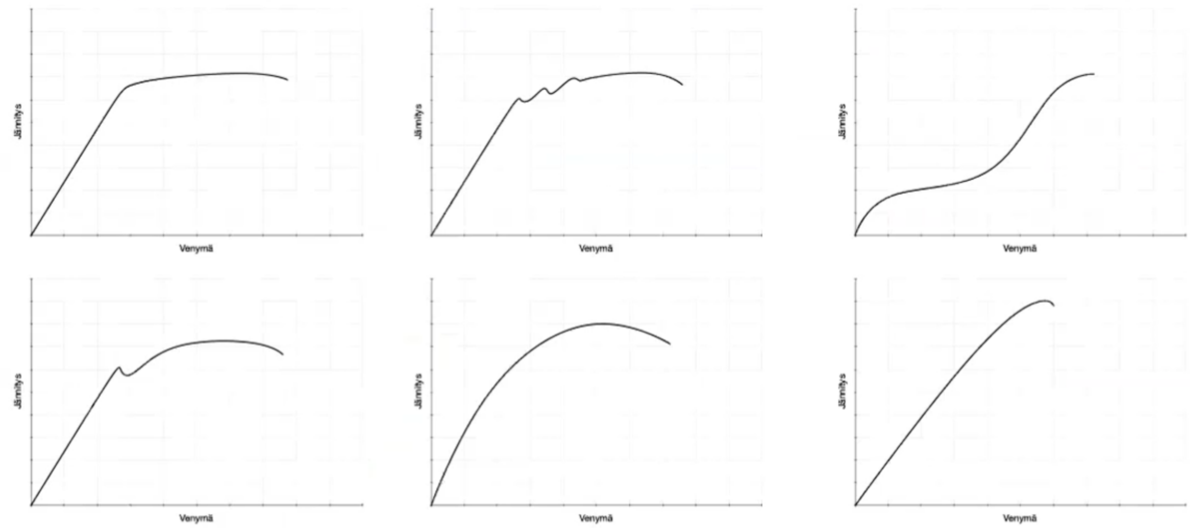

Ductility

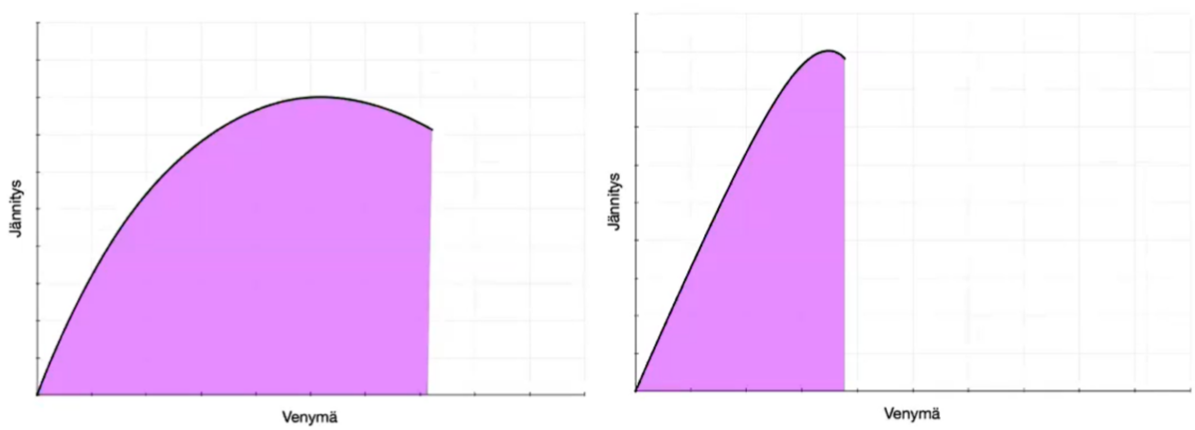

Notch strengthening

Notch turn uniaxial stress to triaxial stress
Material inside notch behaves as if it's stronger

E.g. Brazing / soldering

Macroscopic approximation

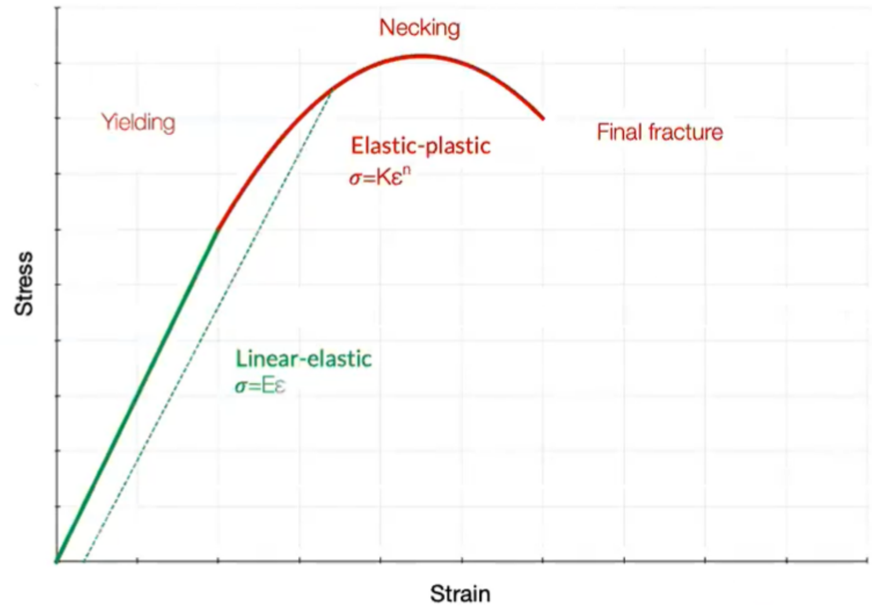

Aalto-yliopisto
Insinööritieteiden
korkeakoulu

High temperature behaviour of materials

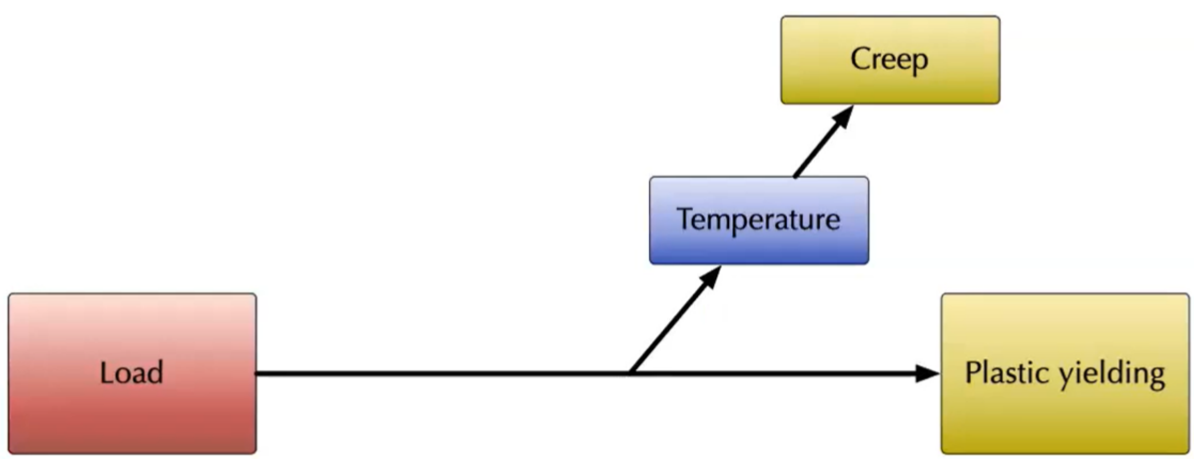

High temperature deformation

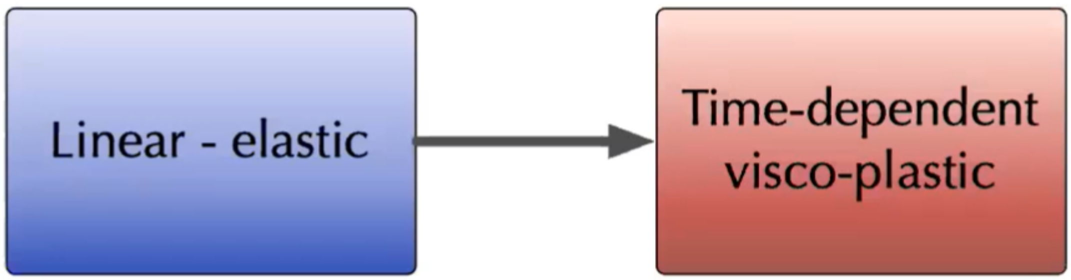

Spring-Dashpot model

$$\varepsilon = \frac{\sigma}{R}$$

$$\dot{\varepsilon} = \frac{\sigma}{\eta}$$

$$\varepsilon = \frac{\sigma\, t}{\eta}$$

Energy losses in cyclic loading

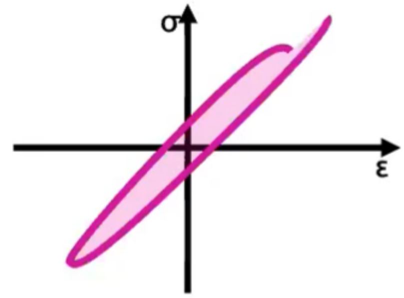

$$\sigma = \Re\left\{\sigma_0 e^{(i\omega-\zeta)t}\right\}$$
$$\varepsilon = \Re\left\{\varepsilon_0 e^{(i\omega-\zeta)t}\right\}$$

$$\Delta U = \oint \sigma d\varepsilon$$

$$\eta = \frac{D}{2\pi} = \frac{1}{Q} \asymp \frac{\Lambda}{\pi} = 2\zeta$$

Visco-plastic deformation: creep

$$\varepsilon(t) = C(t)\ \sigma$$

Elastic deformation

t

- instant
- reversible

Plastic deformation

- irreversible
- strain rate dependent

Primary creep

- changing
- creep rate decreases with time

Secondary creep

- constant-rate

Tertiary creep

- creep rate increases
- related to accumulating damage

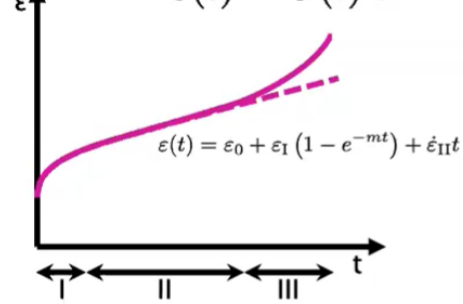

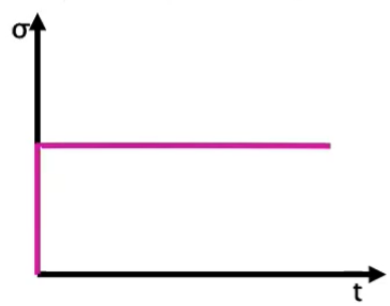

Stress relaxation

In strain (displacement) control creep decreases stresses

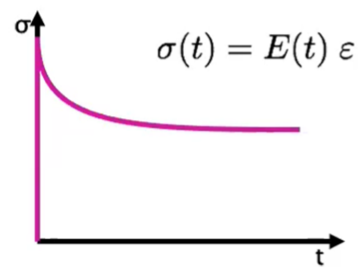

Thermally activated plastic deformation

Creep

Numerous mechanisms

Creep

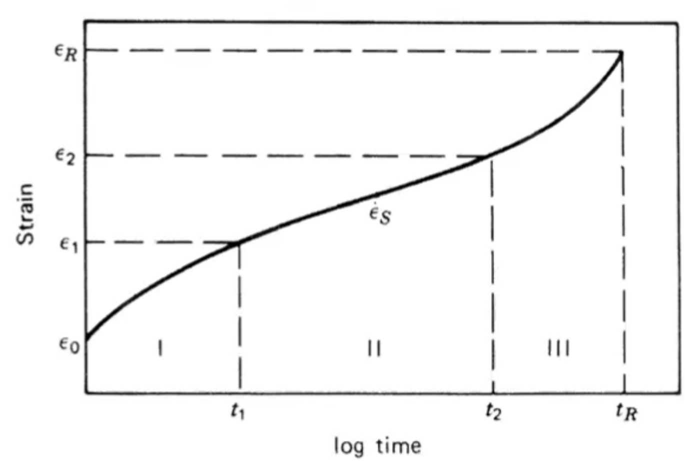

Creep is life-limiting mechanism in

Power plants
Oil refineries
Turbine blades
...

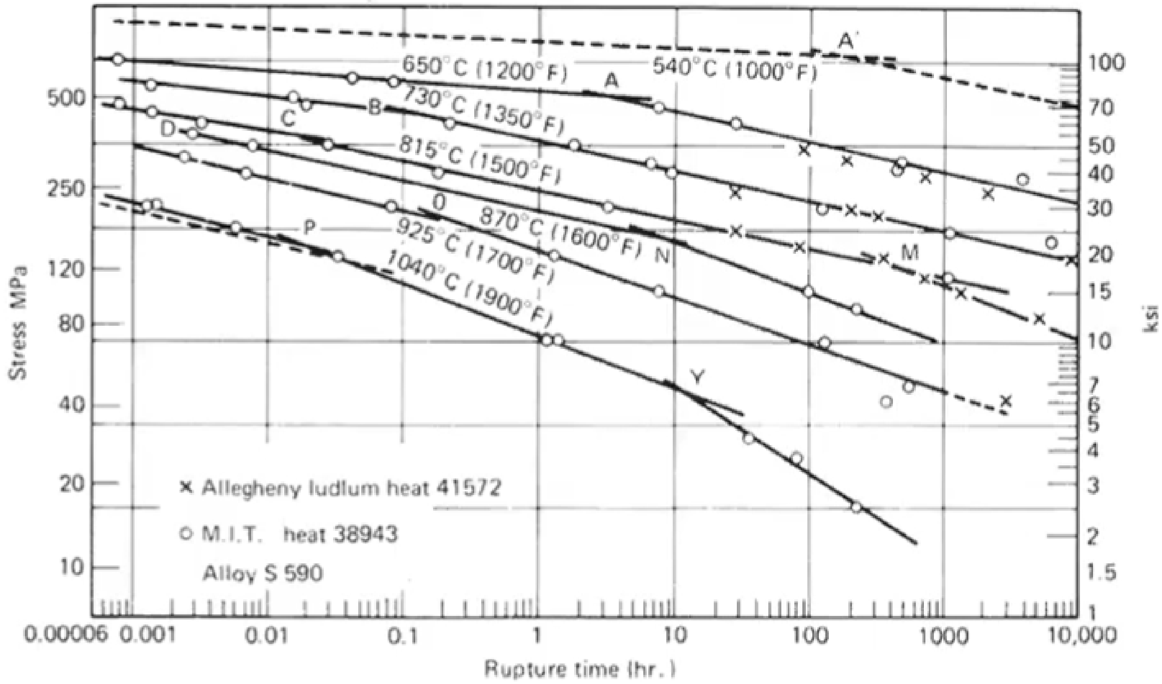

FIGURE 5.3 Stress–rupture life plot at several test temperatures for iron based alloy S-590. (From N. J. Grant and A. G. Bucklin, copyright American Society for Metals, Metals Park, OH, © 1950.)

Activation energy

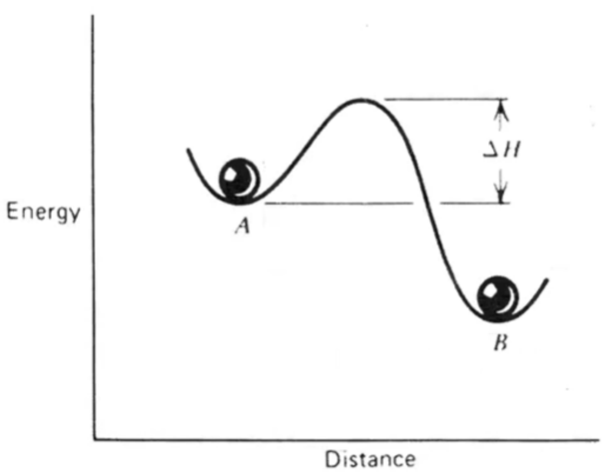

$$\dot{\varepsilon} = Ae^{-Q}$$

Mechanisms

Stress driven, thermally assisted deformation

Several mechanisms

- Each with their own activation energy
- With increasing temperature, mechanisms with higher activation energy become active
- Largest strain rate dominates

Mechanisms

Activation of dislocation sources

Overcoming Peiers stress

"jogs"

Assisted dislocation climb

Movement of Cottrell clouds with diffusion

Diffusion creep

- Cobble
- Nabarro-Herring

Dislocation creep

High stress, low temperature

Diffusion assisted dislocation movement over barriers

Dislocation creep

Power law -creep

- $10^{-4}\,G \lesssim \sigma \lesssim 10^{-2}\,G$
- Dislocation movement assisted by diffusion
- Balance between strain hardening and recovery
- Dislocation climb
- Stress increases driving force and dislocation density

Dislocation glide

- $10^{-2}\,G \lesssim \sigma$

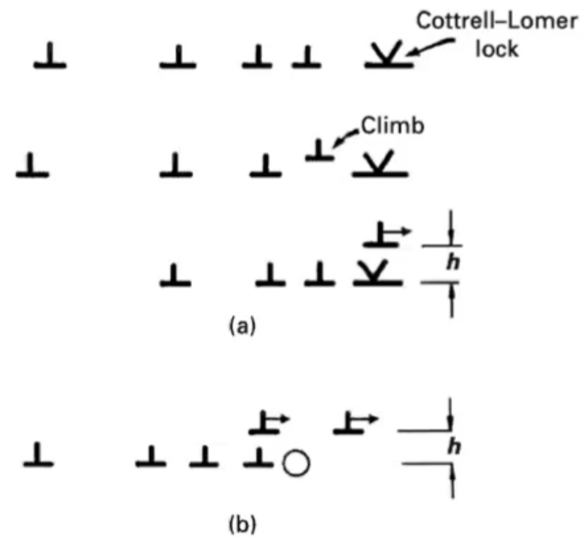

Diffusion creep

High temperature, small stress
Vacancies gather in tensile stress zones
Diffusion controlled

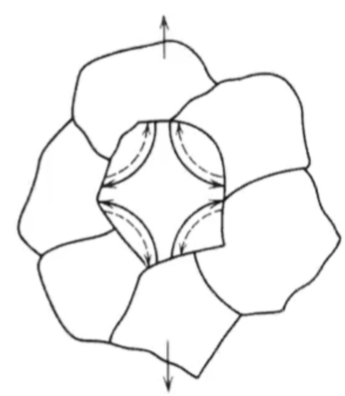

Grain boundary mechanisms

Coble

- Gliding due to fast grain boundary diffusion

Nabarro-Herring

- Grain boundaries act as sources (sinks) of vacancies
- Vacancies diffuse through grains

Both are grain size dependent

Dominating in small stresses (high temperatures)

- $\sigma \lesssim 10^{-4}\,G$

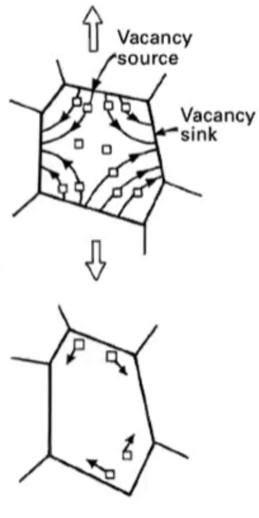

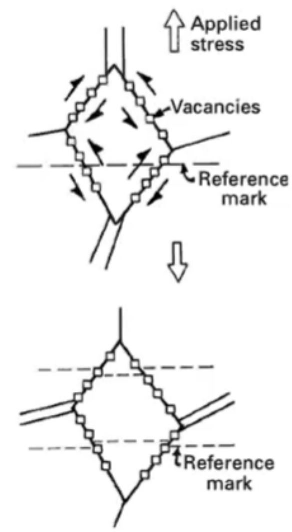

$$\dot{\varepsilon}_{\mathrm{NH}} = A_{\mathrm{NH}} D \frac{Gb}{k_{\mathrm{B}}T} \left(\frac{b}{d}\right)^2 \left(\frac{\sigma}{G}\right)$$

$$\dot{\varepsilon}_{\mathrm{C}} = A_{\mathrm{C}} D_{\mathrm{gb}} \frac{Gb}{k_{\mathrm{B}}T} \left(\frac{\delta}{b}\right) \left(\frac{b}{d}\right)^3 \left(\frac{\sigma}{G}\right)$$

Grain boundary sliding

To preserve material integrity, grain boundaries must slide

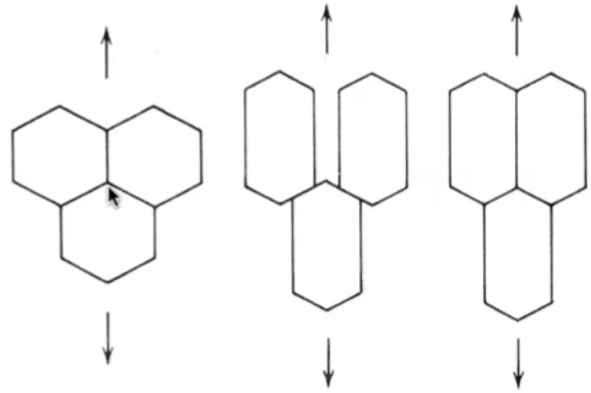

(a) (b) (c)

Creep failure

Grain boundaries open
Opening grain boundaries form cracks
Cracks increase local stress

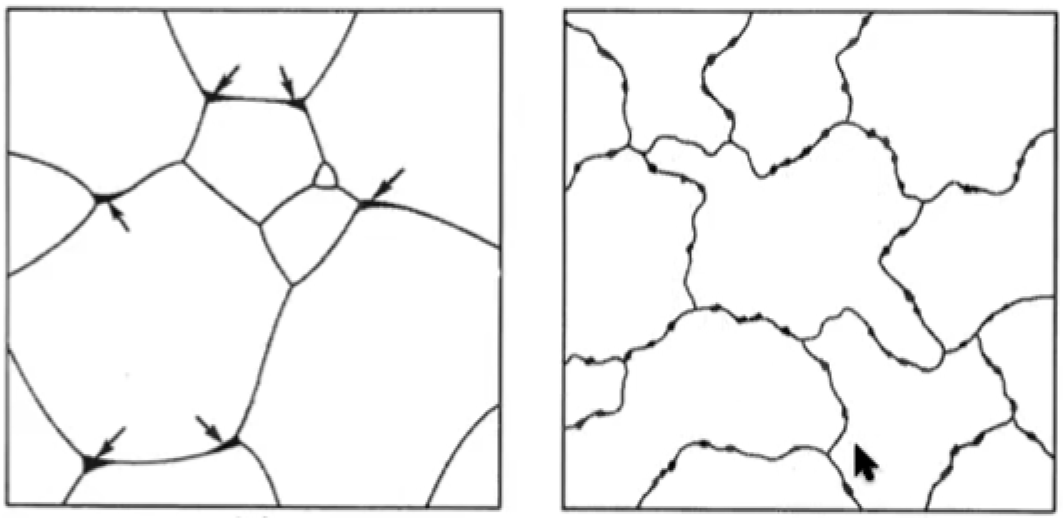

(A) (B)

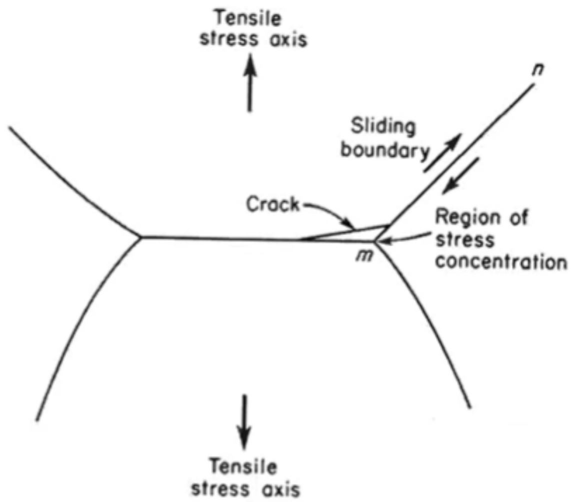

Fig. 23.29 Zener's method for the formation of wedge-shaped cavities. Sliding along the boundary *mn* relaxes the shear stress along the boundary and concentrates the stress at the grain corner.

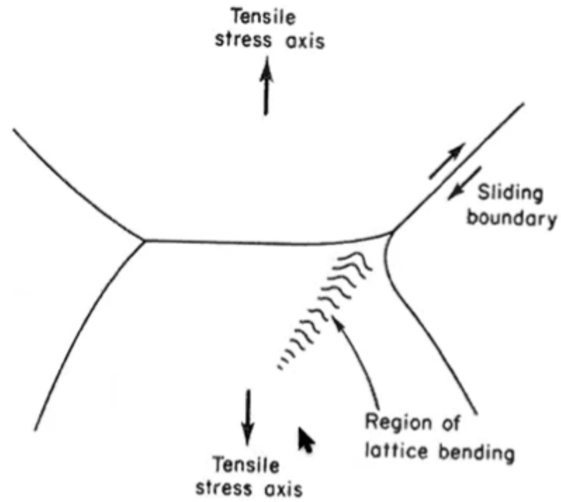

Fig. 23.30 The stress concentration at a grain corner may be relieved by plastic deformation in the grain ahead of the sliding boundary.

Fig. 23.31 A double fold on the surface of a 20 percent Zn-Al creep specimen tested at 500°F and 2300 psi. 75X. (Chang, H. C., and Grant, N. J., *Trans. AIME*, **206** 544 [1956].)

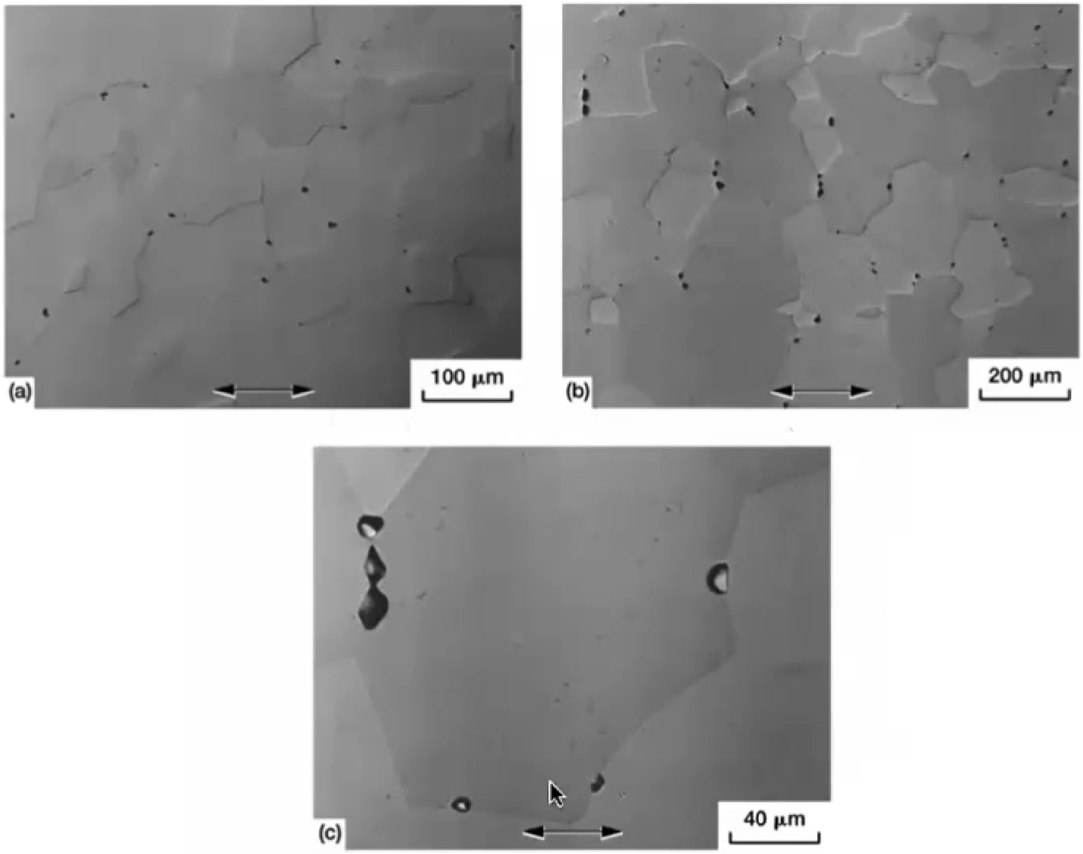
(a)
100 μm
(b)
200 μm
(c)
40 μm

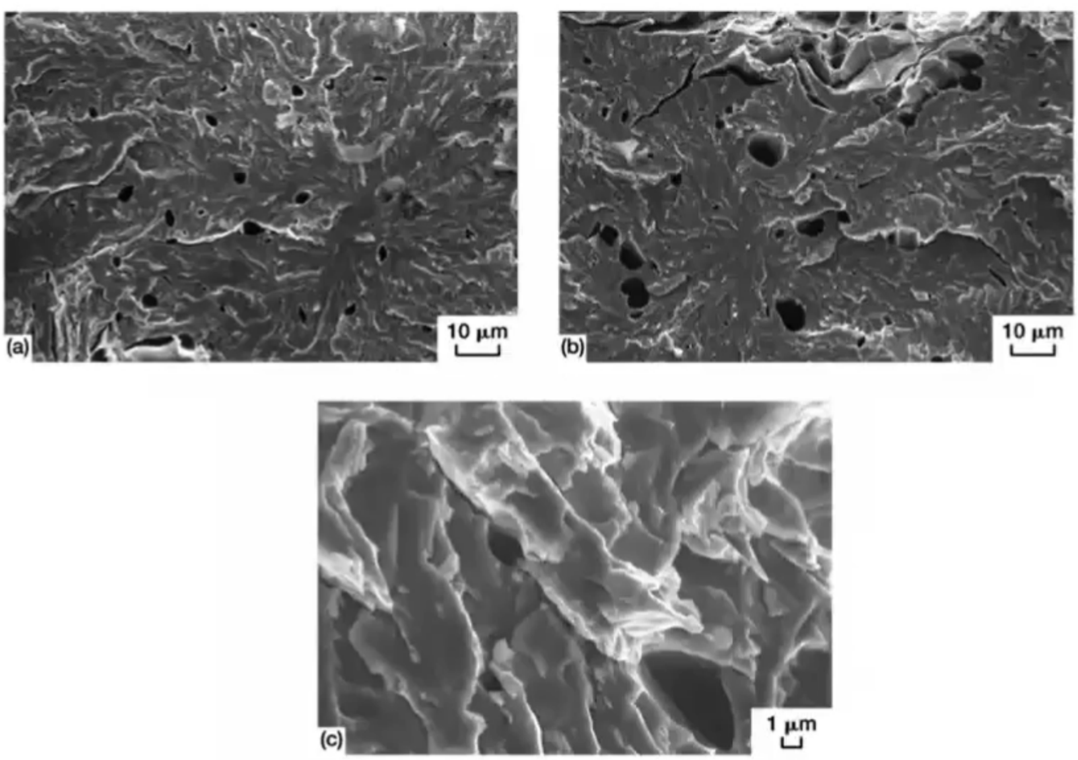
(a)
10 μm
(b)
10 μm
(c)
1 μm

Direct observation in electron microscopy

- Digital Image Correlation and Electron BackScatter Diffraction

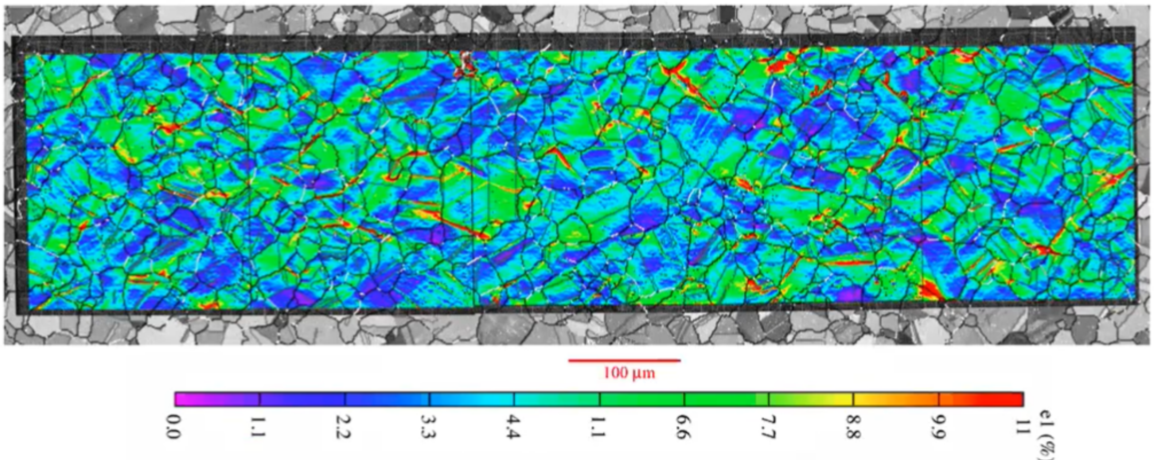

Superplasticity

Some materials

- small grain size

Certain strain-rate / temperature region

Large deformations attainable

>1000%

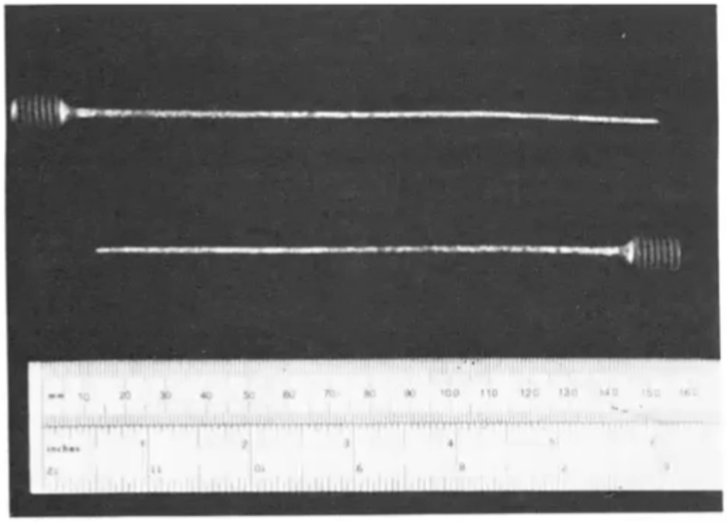

Deformation map

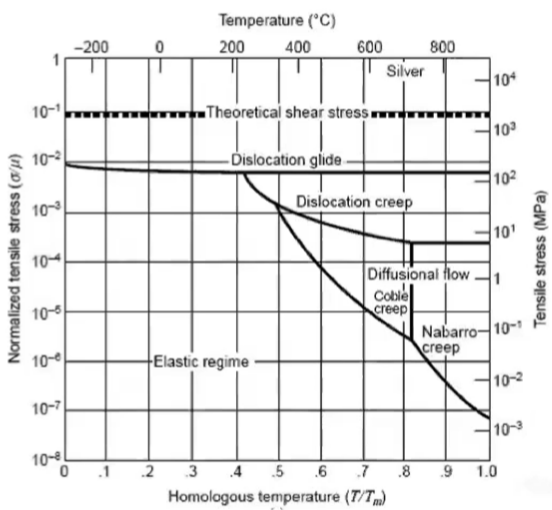

Grain boundary dependence

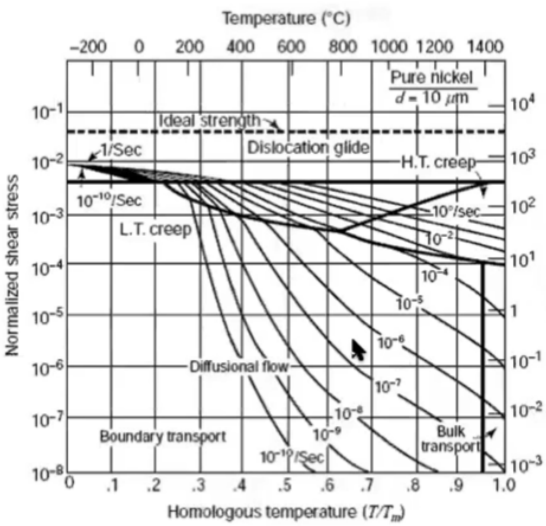

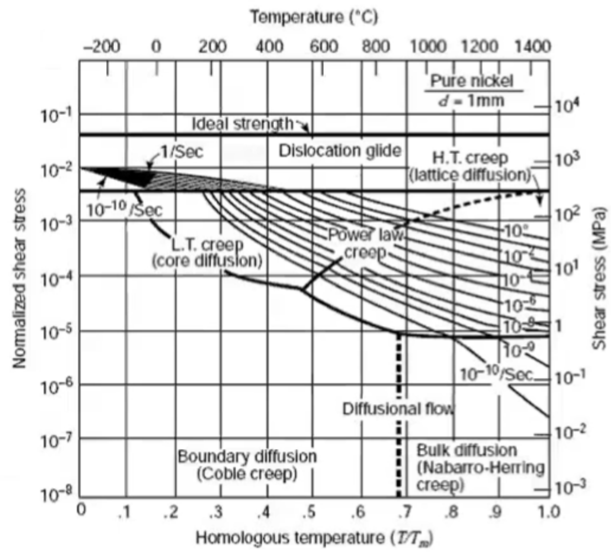

Design

Testing is time consuming

Accelerated testing is difficult

- higher temperature or higher stress
- different mechanism activates

Unified parameter to correlate behavior in different regions

Several (conflicting) parameters proposed

Larson - Miller

Do testing in high temperature (fast)

Use material in lower temperature (where service time is long)

For given stress, correlate time-to-rupture in different temperatures with Larson-Miller parameter

Larson-Miller parameter

Activation energy ΔH

- Driving force depends from stress
- Activation energy may be stress dependent

$$\text{rate} \sim Ae^{\frac{\Delta H}{RT}}$$

$$\frac{\Delta H}{R} = T\left(C - \log(t)\right)$$

$$C = \log(A) \approx 20$$

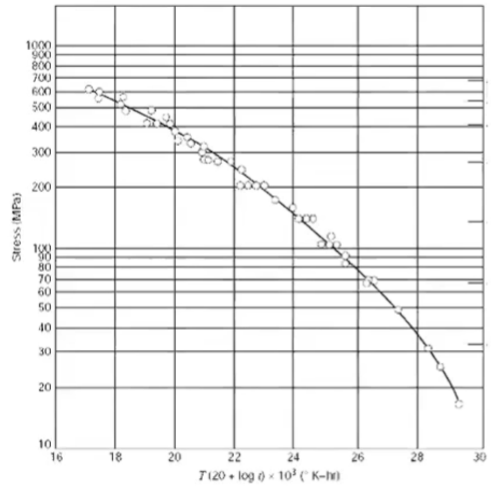

Creep activation energy close to diffusion activation energy

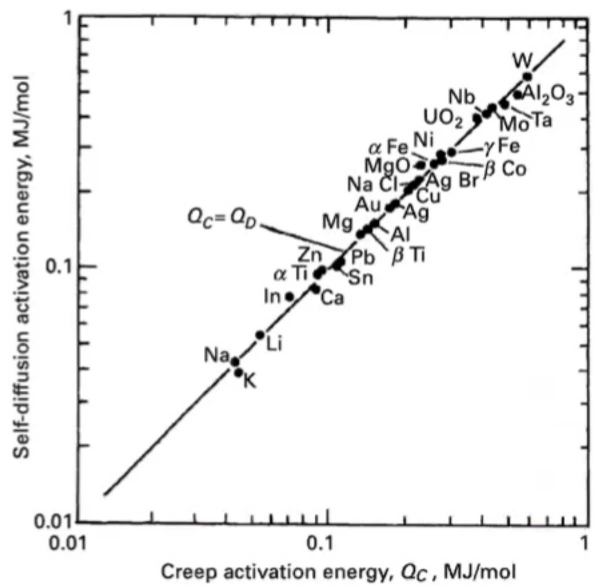

High temperature materials

High melting point
High temperature precipitates (dispersions)
Large grain size (!)

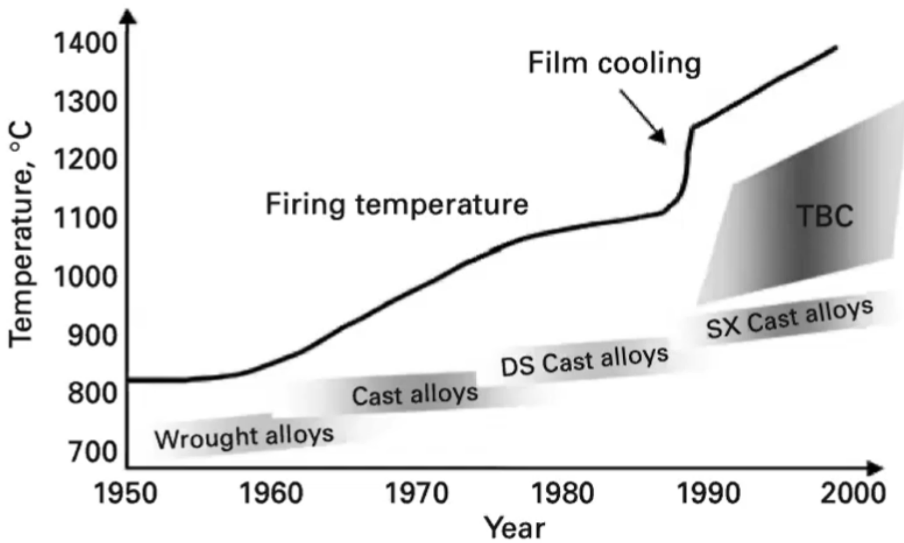

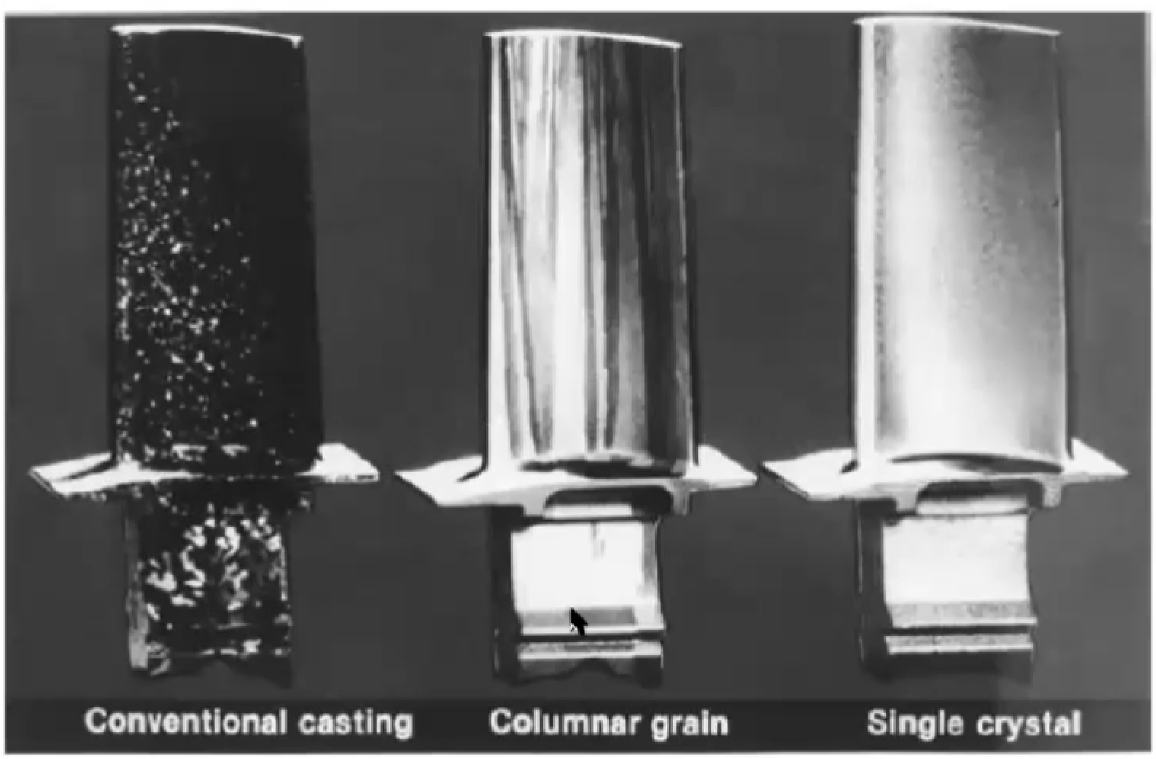

Case

Example of current development

Alloy design of creep resistant 9Cr steel using a dispersion of nano-sized carbonitrides

Int. J. of Pressure Vessels and Piping
F. Abe, M. Taneike, K. Sawada
84 (2007), 3-12

Target: Ultra-super-critical power plants

lower CO_2
higher temperature >650° C
old materials insufficient

=> better oxidation resistance and creep resistance

Significant factors

Dispersion strengthening

- inversely proportional to the mean inter-particle distance
- proportional to the volume fraction

conventional 9 to 12Cr steels such as

- P91 (9Cr–1Mo–VNb steel),
- P92 (9Cr–0.5Mo–1.8W–VNb steel) and
- P122 (11Cr–0.4Mo–2W–CuVNb steel)

tempered martensite
high density of dislocations and fine precipitates
M23C6 carbides rich in chromium and MX carbonitrides

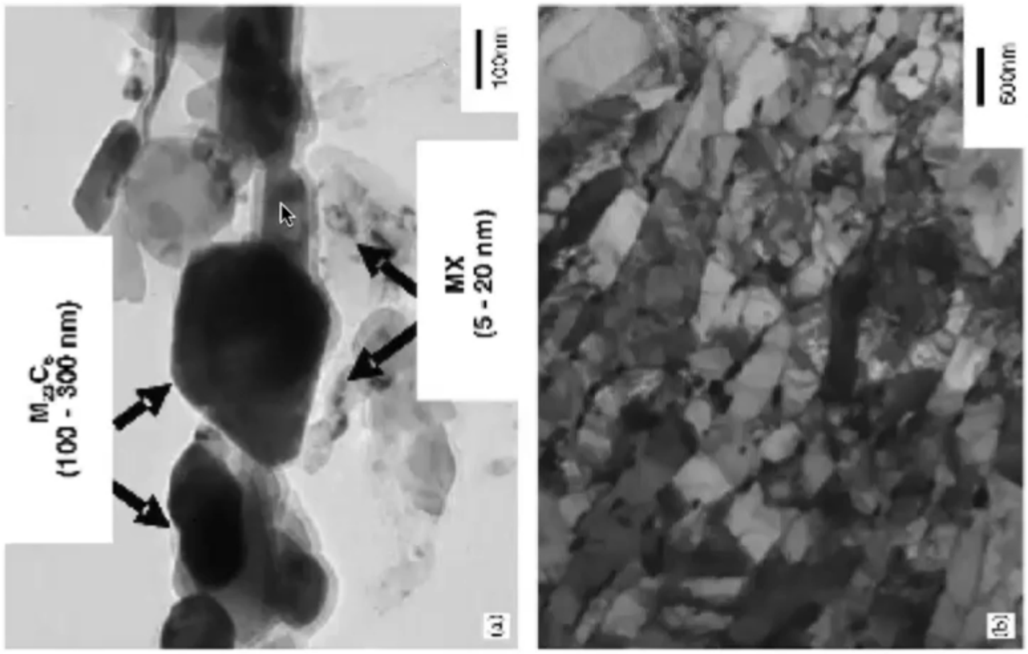
$M_{23}C_6$
(100 - 300 nm)
MX
(5 - 20 nm)
100nm
500nm
(a)
(b)

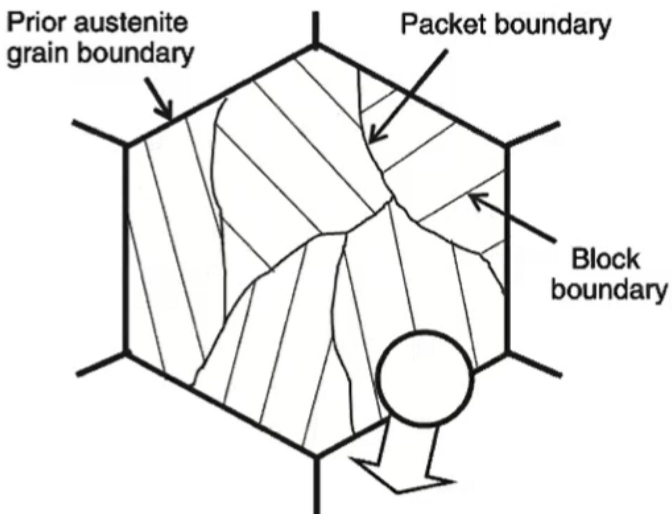
Prior austenite
grain boundary
Packet boundary
Block
boundary

(a)

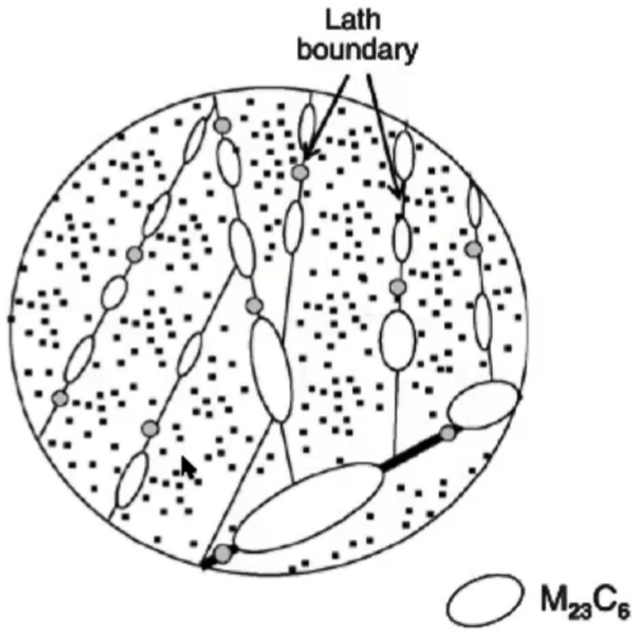

(b)

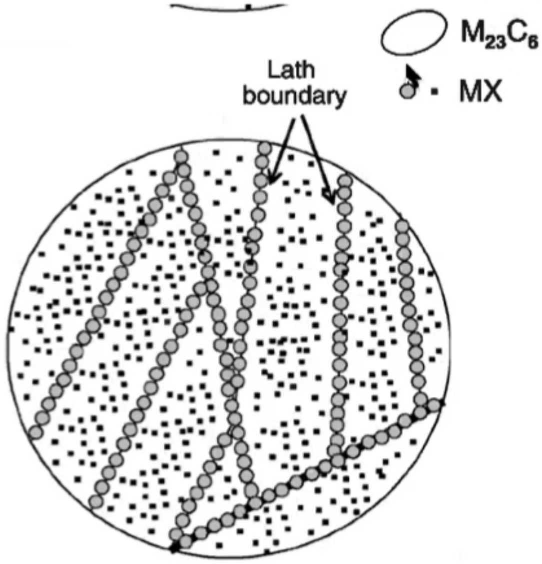

(c)

Table 1
Chemical compositions and heat treatment conditions of carbon series of 9Cr–3W–3Co–VNb–0.05N steels with different carbon concentration

	C	Si	Mn	Cr	W	V	Nb	Co	N (mass %)	B	Normalizing	Tempering
0.002C	0.002	0.29	0.51	9.19	2.96	0.20	0.060	3.09	0.049	0.0070	1100 °C × 0.5 h	800 °C × 1 h
0.018C	0.018	0.29	0.50	9.16	2.91	0.20	0.058	2.94	0.050	0.0058	1100 °C × 0.5 h	800 °C × 1 h
0.047C	0.047	0.30	0.51	9.24	2.90	0.20	0.059	3.07	0.050	0.0063	1100 °C × 0.5 h	800 °C × 1 h
0.078C	0.078	0.31	0.51	9.26	2.93	0.20	0.061	3.08	0.049	0.0064	1100 °C × 0.5 h	800 °C × 1 h
0.12C	0.120	0.30	0.50	9.27	2.93	0.20	0.058	3.08	0.048	0.0065	1100 °C × 0.5 h	800 °C × 1 h
0.16C	0.160	0.30	0.51	9.26	2.94	0.20	0.058	3.08	0.047	0.0061	1100 °C × 0.5 h	800 °C × 1 h

Table 2
Chemical compositions and heat treatment conditions of nitrogen series of 9Cr–3W–3Co–VNb–0.002C steels with different nitrogen concentration

	C	Si	Mn	Cr	W	V	Nb	Co	N (mass %)	B	Normalizing	Tempering
0.05N	0.0020	0.29	0.51	9.19	2.96	0.20	0.060	3.09	0.049	0.0070	1100 °C × 0.5 h	800 °C × 1 h
0.07N	0.0019	0.30	0.50	8.84	3.02	0.20	0.059	3.02	0.074	0.0066	1200 °C × 0.5 h	790 °C × 4 h
0.10N	0.0020	0.29	0.53	8.87	2.90	0.19	0.060	3.03	0.103	0.0062	1200 °C × 0.5 h	790 °C × 4 h

Table 3
Chemical compositions and heat treatment conditions of Ti series of 9Cr–2W–VNb–0.13C steels with and without 0.05Ti

	C	Si	Cr	W	V	Nb	Co	N (mass %)	Normalizing	Tempering
0Ti	0.13	0.51	8.49	1.93	0.195	0.045	<0.001	0.006	1100 °C × 1 h	760 °C × 1 h
0.05Ti-S	0.13	0.50	8.42	1.91	0.192	0.044	0.047	0.006	1100 °C × 1 h	760 °C × 1 h
0.05Ti-H	0.13	0.50	8.42	1.91	0.192	0.044	0.047	0.006	1300 °C × 1 h	770 °C × 1 h

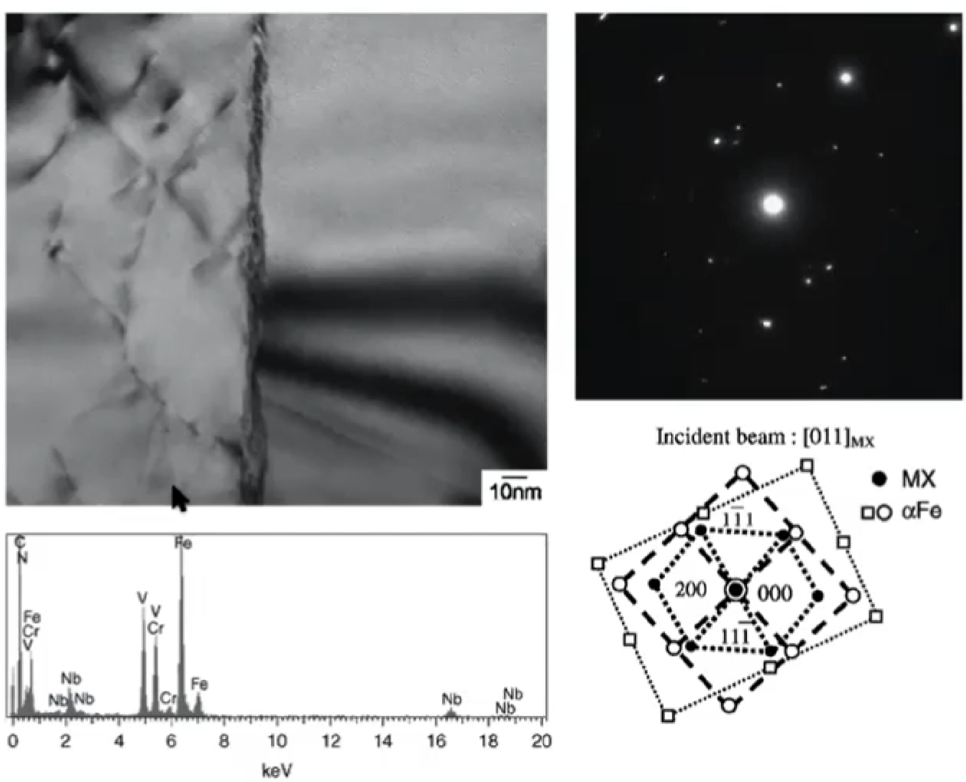

Fig. 5. Nano-size MX precipitates along boundaries in 0.002C steel in Table 1, after tempering.

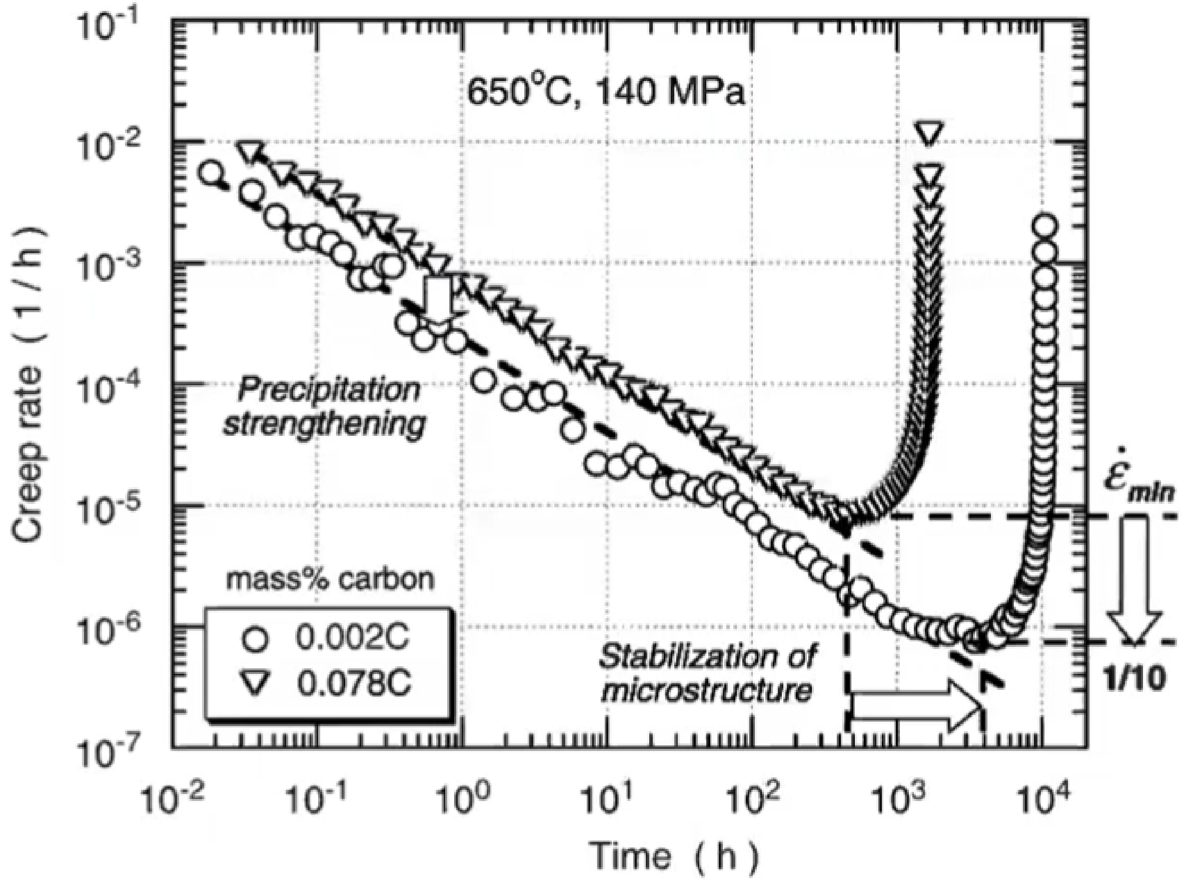

Fig. 7. Creep rate versus time curves of 0.002C and 0.078C steels in Table 1 at 650 °C and 140 MPa.

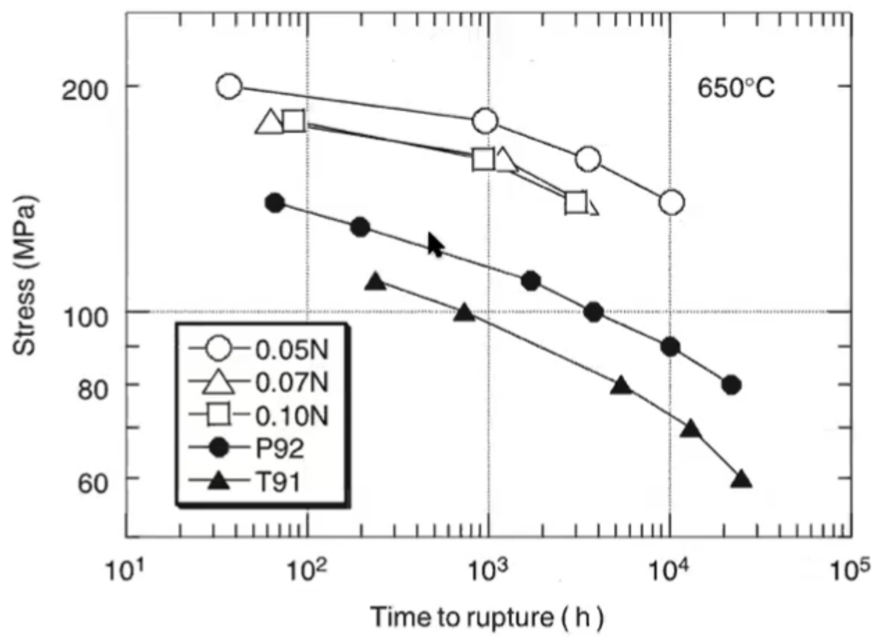

Fig. 8. Creep rupture data for the 0.05N, 0.07N and 0.10N steels in Table 2 at 650 °C, comparing with those for conventional steels P92 and T91.

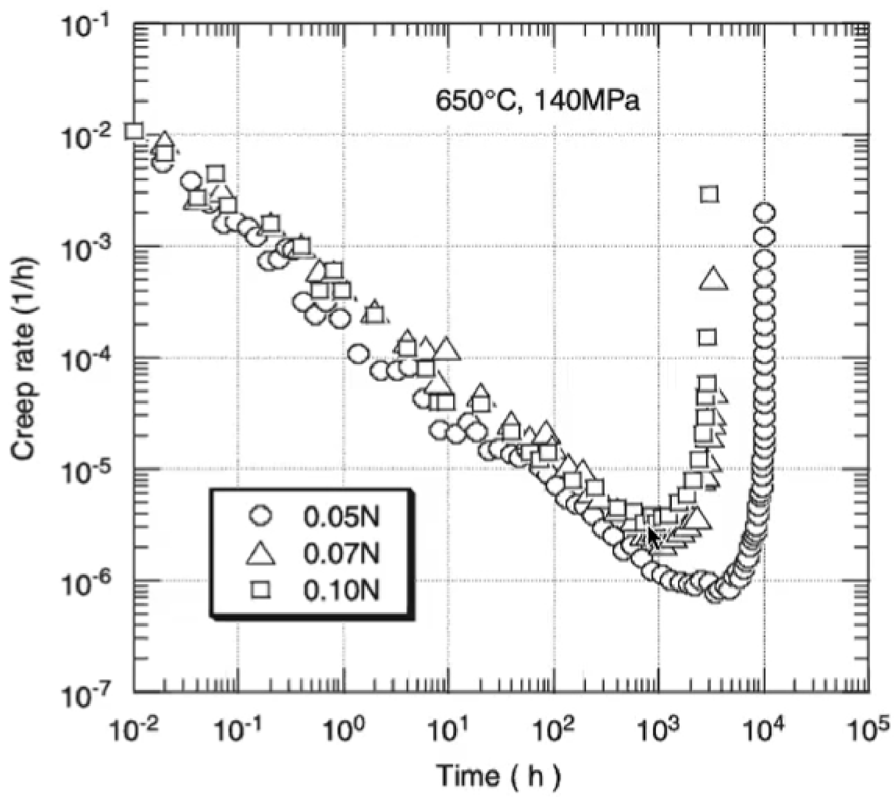

Fig. 10. Creep rate versus time curves of the 0.05N, 0.07N and 0.10N steels in Table 2 at 650 °C and 140 MPa.

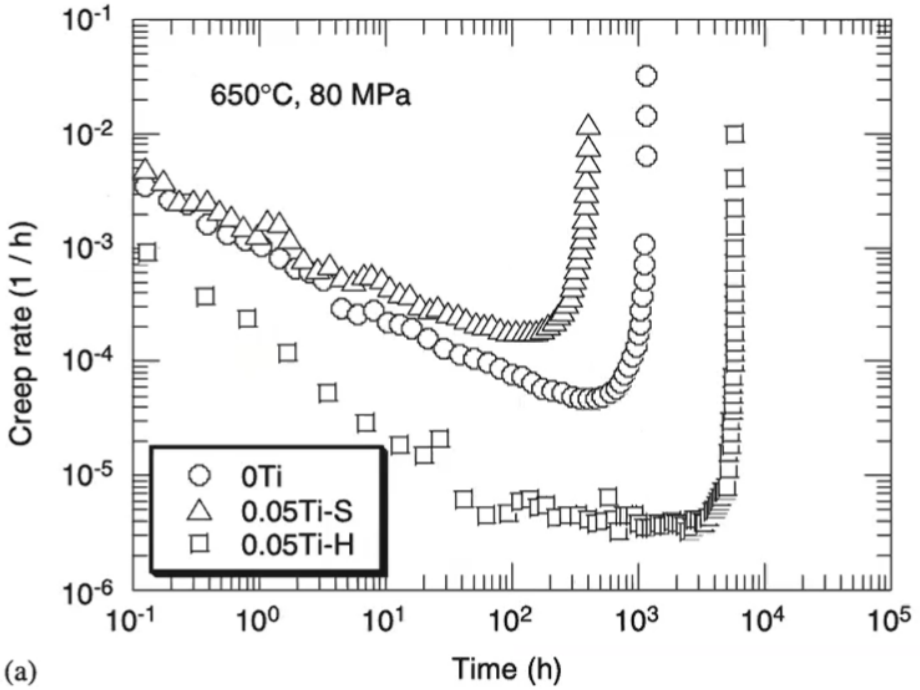

650°C, 80 MPa
Creep rate (1 / h)
Time (h)
0Ti
0.05Ti-S
0.05Ti-H

(a)

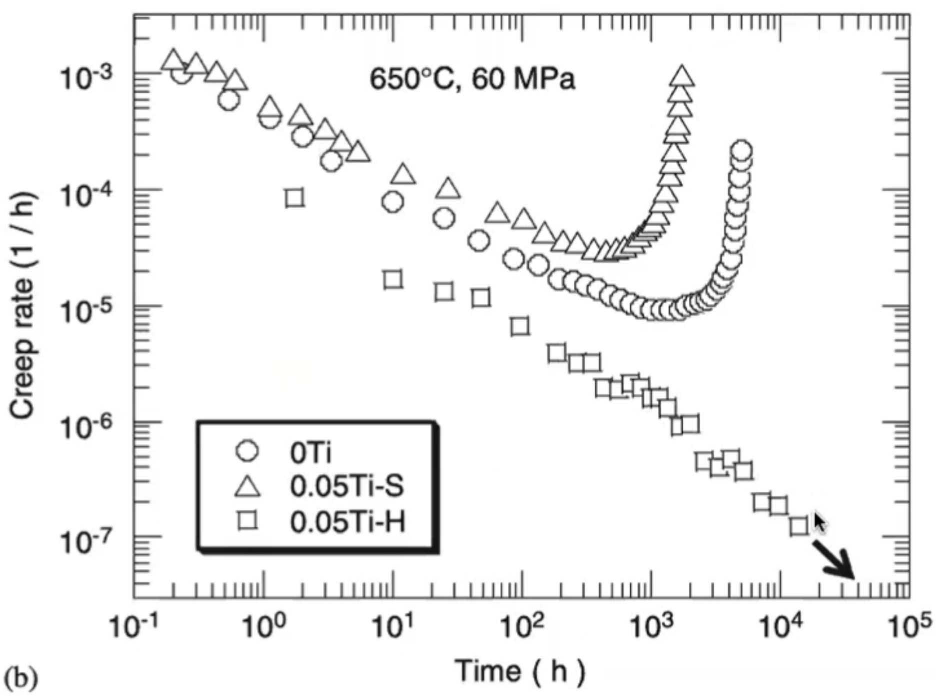

650°C, 60 MPa
Creep rate (1 / h)
Time (h)
0Ti
0.05Ti-S
0.05Ti-H

(b)

Conclusion

MX-nitrides in grain boundaries improve creep strength (attained by lower carbon content)

Increased nitride decreases creep strength (MX nitrides change to coarser Z-phase)

TiC carbides increase creep strength in low stresses

Engineering Failure Analysis 18 (2011) 1407–1414

Contents lists available at ScienceDirect

Engineering Failure Analysis

journal homepage: www.elsevier.com/locate/engfailanal

ELSEVIER

Creep failure of low pressure turbine blade of an aircraft engine

N. Ejaz *, I.N. Qureshi, S.A. Rizvi

Institute of Industrial Control Systems, P.O. Box 1398, Rawalpindi, Pakistan

Detection

After overhaul, changes and sound and vibrations were noticed

Visual examination showed cracks

Blade had seen 270 hours of use

Root cause analysis of failure and comparison to unbroken blade

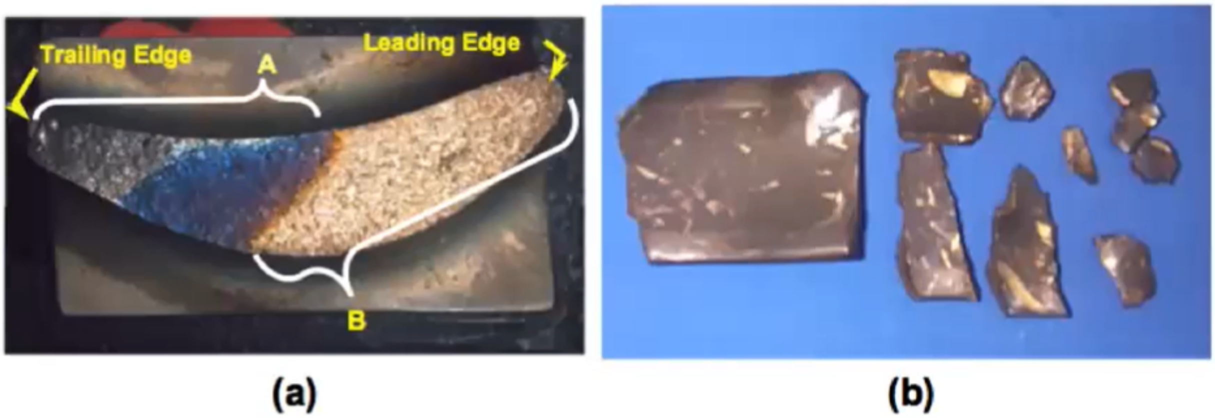

Fig. 1. Failed blade, (a) fracture surface, (b) remains of the airfoil.

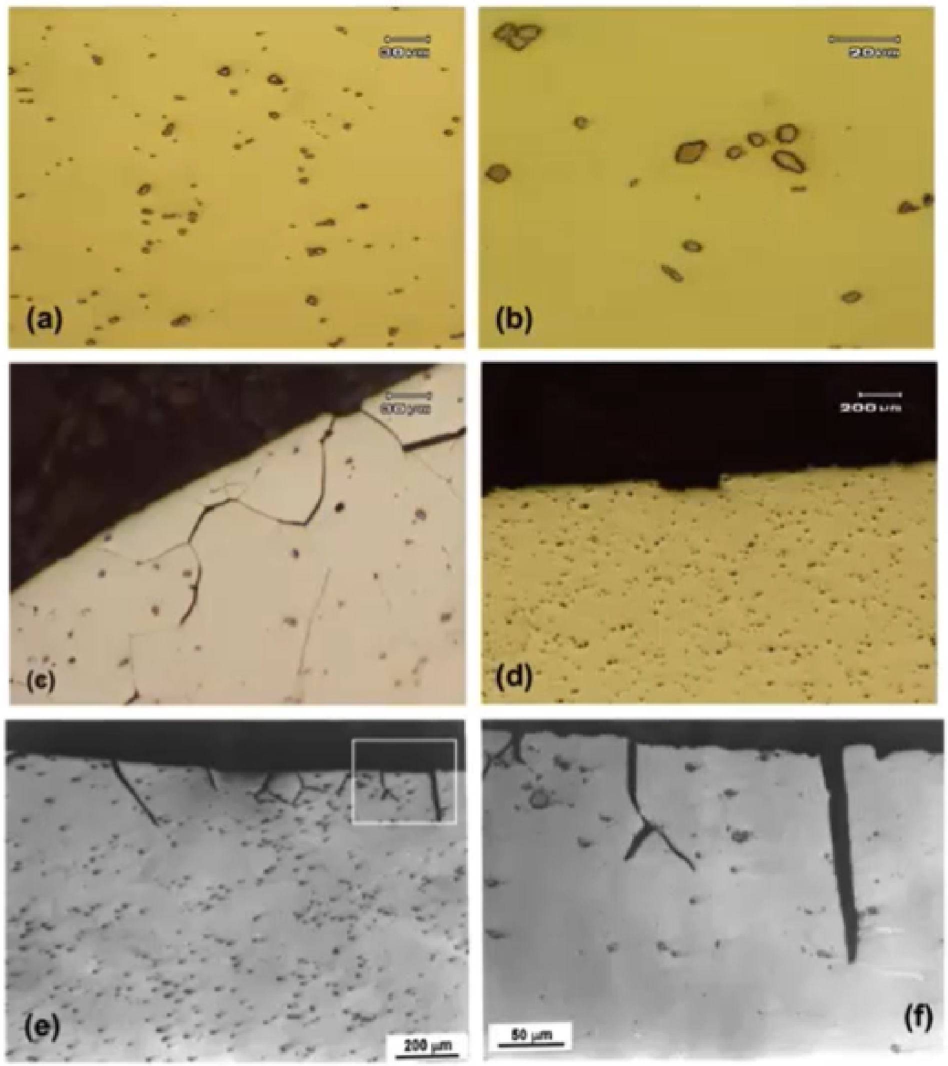

Fig. 3. Polished sample of failed blade, (a) revealing primary carbides, (b) same as (a) at high magnification, (c) cracks at the grain boundaries at region 'C' (see Fig. 2), (d) region 'B', (e and f) neighboring blade at region 'C'.

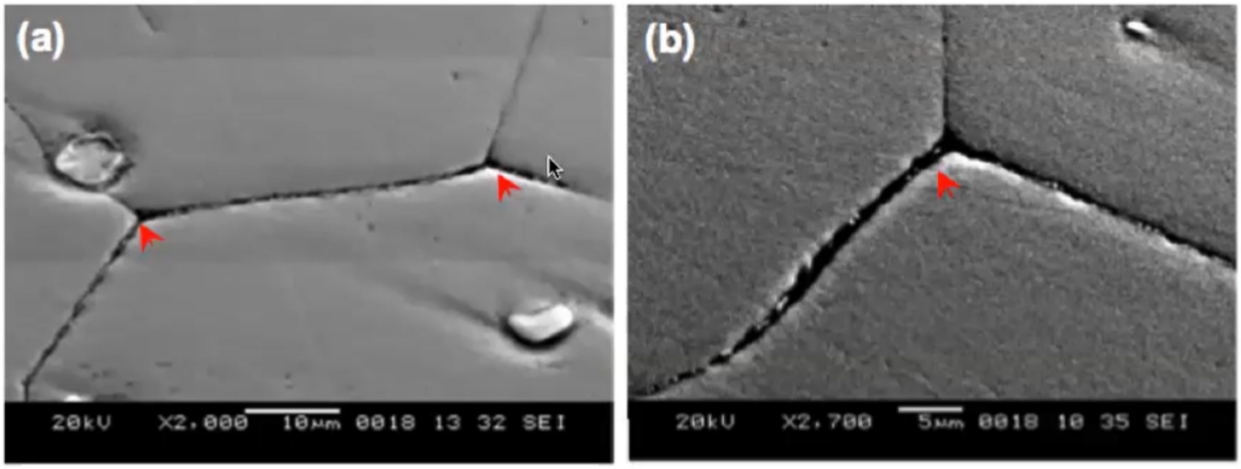

Fig. 5. Triple point wedge type cracks near the root region of airfoil in, (a) failed blade, (b) adjacent unfailed blade.

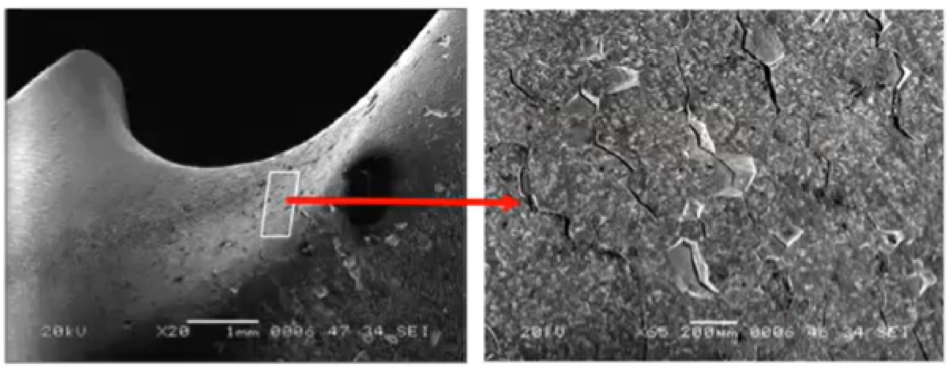

Fig. 6. Opened cracks with dropped grains at the 'C' region of an unfailed blade.

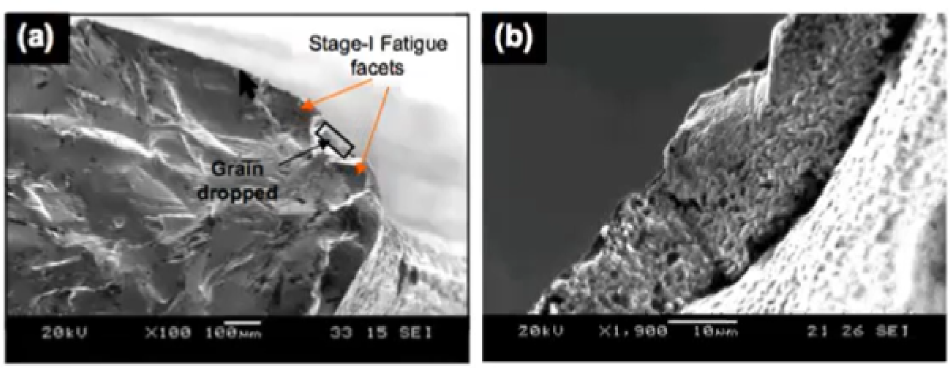

Fig. 7. Failed blade fractured surface revealing crack initiation from a dropped grain region as well as stage-I fatigue facets; (b) is the high magnification of boxed region in the (a).

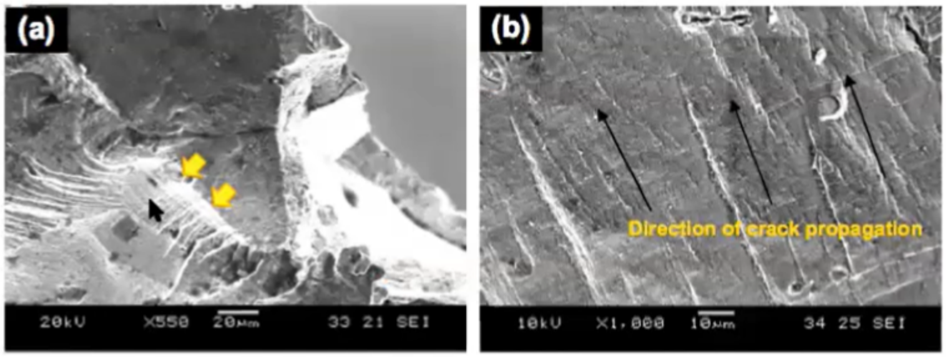

Fig. 8. Failed blade fractured surface showing start of stage-II fatigue, (a) fatigue striations (arrows) next to the stage-I fatigue along with tear ridges, (b) high magnification showing striations and tear ridges.

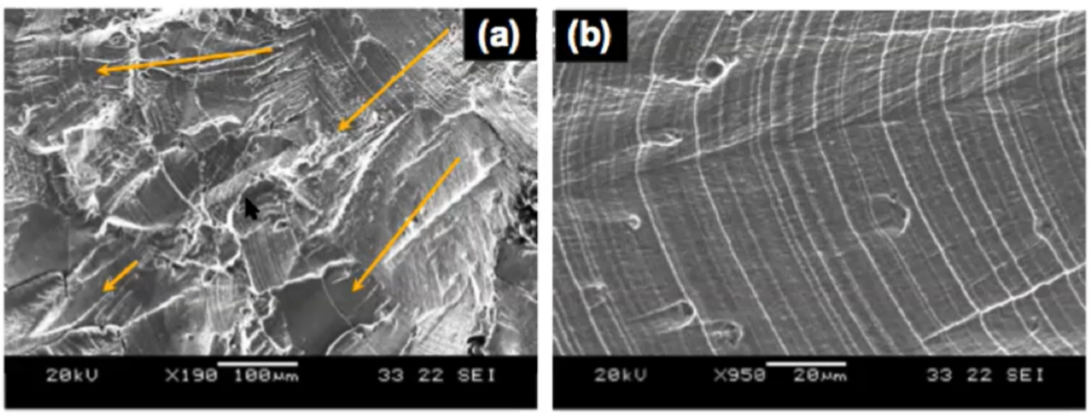

Fig. 9. Failed blade; fractured surface revealing coarse striations near overload region, (a) low magnification, (b) high magnification.

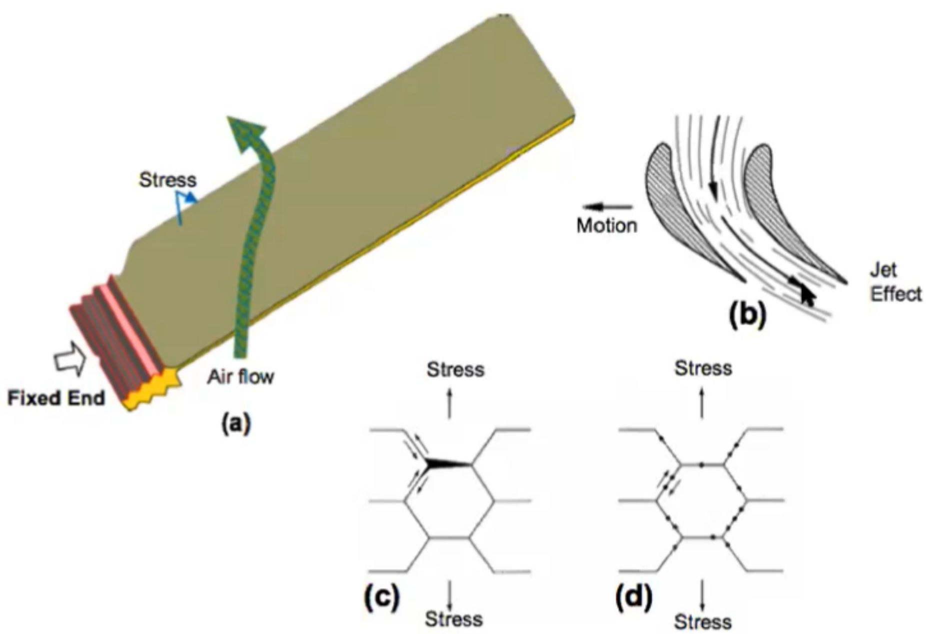

Fig. 11. Schematic revealing, (a) blade pressure side, (b) movement of the gases and motion of the turbine, (c and d) triple point cracking and cavitation, respectively in intergranular creep; small arrows show the grain boundary sliding direction.

Discussion

Rims had been grinded

OEM-guidance required rim grinding of 1 mm after certain number of hours (!)

Failure started from "triple point creep crack"

Neighboring unbroken blades had similar starter cracks

Failure continued with fatigue (crack growth)

Chain of events

Wedge-like triple point creep cracks nucleated on the tail-edge

Creep cracks nucleated fatigue cracks

Fatigue cracks grew with high-cycle fatigue driven by vibrations

Cracks grew to critical dimension and caused final fracture of the blade

Conclusions

The primary cause of the failure was creep cracking

Thermally caused microstructural weakening was cited as contributing factor

Blade grinding has changed blade geometry and may have increased loading

Engine service history (higher than expected loads) may have contributed to the failure

Note: no macroscopic plastic deformation